SLAC-PUB-8694
November, 2000

Quadrupole Misalignments and Steering in Long Linacs*

G. V. Stupakov
Stanford Linear Accelerator Center, Stanford University, Stanford, CA 94309

Abstract

The emittance dilution of a relativistic beam in a long linear accelerator caused by quadrupole misalignments is studied. First, an analytical formula is derived for the emittance dilution due random uncorrelated offsets of the quadrupoles in a FODO lattice for a beam of constant energy. It is shown that there is a critical length of the linac below which the emittance growth scales as N^3 with the number of quadrupoles. For linacs longer than the critical, the emittance dilution scales linearly with N. Analytical results are obtained for the residual emittance growth after lattice alignment as a function of the resolution of the beam position monitors and mover steps. The results are also generalized for a FODO lattice and a beam with slowly varying parameters. They are compared with computer simulations for the NLC.

Submitted to Physical Review Special Topics: Accelerators and Beams

*Work supported by Department of Energy contract DE–AC03–76SF00515.

Quadrupole Misalignments and Steering in Long Linacs

G. V. Stupakov

November 7, 2000

Abstract

The emittance dilution of a relativistic beam in a long linear accelerator caused by quadrupole misalignments is studied. First, an analytical formula is derived for the emittance dilution due random uncorrelated offsets of the quadrupoles in a FODO lattice for a beam of constant energy. It is shown that there is a critical length of the linac below which the emittance growth scales as N^3 with the number of quadrupoles. For linacs longer than the critical, the emittance dilution scales linearly with N. Analytical results are obtained for the residual emittance growth after lattice alignment as a function of the resolution of the beam position monitors and mover steps. The results are also generalized for a FODO lattice and a beam with slowly varying parameters. They are compared with computer simulations for the NLC.

1 Introduction

In this paper we study the emittance dilution of a beam caused by quadrupole misalignments in a long linac. To suppress the beam break-up instability by means of BNS damping [1] an energy spread is usually introduced in the beam. For the Next Linear Collider (NLC) [2], the energy spread within the bunch will be of order of 1%. Due to the lattice chromaticity, the deflection of the beam by displaced quadrupoles results in the dilution of the phase space and the growth of the projected emittance.

The effect of lattice misalignments has been previously studied in many papers. A qualitative analysis and main scalings were obtained in Ref. [3],

and detailed studies with intensive computer simulations are described in Ref. [4]. Lattice misalignments caused by the ground motion were analyzed in [5, 6].

The purpose of this paper is to develop a simple model based on a FODO lattice approximation for the linac which allows an analytic calculation of the emittance dilution. With a simple generalization, we also include in the model a slow variation of the lattice parameters, as well as variation of both beam energy and the energy spread. We hope that this analysis can be a useful addition to the standard computer simulations that are typically utilized for the study of the misalignments and orbit correction.

Throughout this paper we assume that the number of quadrupoles in the linac is large, $N \gg 1$, and neglect terms of the relative order of N^{-1} in the calculations. For future linear colliders with the center of mass energy in the range of 1 TeV, typically $N \sim 10^3$, and this is a very good approximation.

The paper is organized as follows. In Section 2 we introduce notation for the parameters of a FODO lattice, and in Section 3 we study the beam orbit in a lattice with randomly misaligned quadrupoles. In Section 4 we find the chromatic emittance growth, and in the next Section we show that, for a given energy spread in the beam, the result is limited to not very long linacs. In Section 6 we study the beam based alignment with account of BPM errors and finite step of the quadrupoles movers. In Section 7 we generalize our results for the case of slow variation of lattice and beam parameters, and in Section 8 we compare the theoretical predictions with computer simulations for the NLC lattice. The last section summarizes the main results of the paper.

2 Beam Orbit in Misaligned Lattice

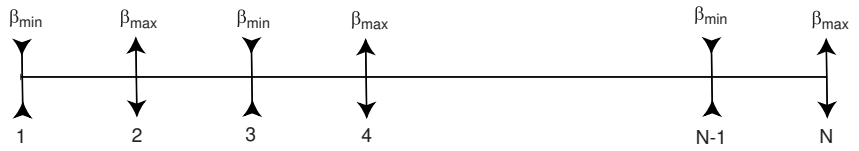

Figure 1: FODO lattice of a linac. Beam positions are measured at the center of each quadrupole.

Let us consider a FODO lattice with a cell length l and a phase advance μ per cell, consisting of N thin quadrupoles as shown in Fig. 1. The focal length of the quadrupoles is equal to $\pm F$ where the positive and negative values of F refer to the focusing and defocusing quadrupoles respectively. We assume that the beam is injected in the linac at the center of the first quadrupole, at $s = 0$, with the zero offset and angle. It propagates through the lattice and the beam emittance is measured at the center of the last, Nth quadrupole. For the beam position (horizontal or vertical) at the locations of the quadrupoles we will use the notation $x_1, x_2, \ldots, x_{N-1}, x_N$, and the orbit angle at the center of the kth quadrupole is denoted by x'_k. The initial conditions for the orbit are $x_1 = x'_1 = 0$.

Note that due to our choice of positions, the derivative of the beta function, and hence the Twiss parameter α, at all locations 1 through N, are equal to zero.

We now assume that each quadrupole in the lattice is misaligned in the transverse direction relative to the axis of the linac by ξ_i, $(1 \leq i \leq N)$, where ξ_i are *random, uncorrelated* numbers. Due to the deflection by misaligned quadrupoles, the original straight orbit will be perturbed. The offset x_i can be found as

$$x_i = \sum_{k<i} R_{12}^{k\to i}\theta_k, \tag{1}$$

where $R_{12}^{k\to i}$ is the $(1,2)$ element of the transfer matrix R and θ_i is the deflection angle resulting from the offset of the ith quadrupole, $\theta_i = \pm\xi_i/F$, for the focusing and defocusing quadrupoles. For brevity, below we will use the notation R_{ik} instead of $R_{12}^{k\to i}$. For R_{ik} we have

$$R_{ik} = \sqrt{\beta_i\beta_k}\,\sin\Delta\psi_{ik}, \tag{2}$$

where the betatron phase advance $\Delta\psi_{ik}$ between kth and ith quadrupoles $(k < i)$ is $\Delta\psi_{ik} = (1/2)(i-k)\mu$.

In what follows, we will also need the orbit angles x'_i where the prime denotes the derivative with respect to the longitudinal coordinate s. For x'_i we have

$$x'_i = \sum_{k\leq i} G_{ik}\theta_k, \tag{3}$$

where again, for convenience, we use the notation $G_{ik} \equiv R_{22}^{k\to i}$, for the $(2,2)$

element of the transfer matrix,

$$G_{ik} = \sqrt{\frac{\beta_k}{\beta_i}} \cos \Delta\psi_{ik}, \tag{4}$$

(note that, due to our choice, $\alpha_i = 0$).

It is convenient to rewrite R_{ik} and G_{ik} in complex notation,

$$R_{ik} = \frac{\sqrt{\beta_i \beta_k}}{2i}(e^{i\Delta\psi_{ik}} - e^{-i\Delta\psi_{ik}}), \qquad G_{ik} = \frac{1}{2}\sqrt{\frac{\beta_k}{\beta_i}}(e^{i\Delta\psi_{ik}} + e^{-i\Delta\psi_{ik}}). \tag{5}$$

3 RMS value for the beam offset

To characterize the deviation of the orbit from the linac axis, we will calculate the average value $\langle x_N^2 \rangle$, where the angular brackets denote averaging over all possible values of ξ. We assume that the average offset $\langle \xi_i \rangle$ vanishes, hence $\langle x_N \rangle = 0$.

For the lattice shown in Fig. 1 the deflection angle θ_k due to the misaligned kth quadrupole is given by the following equation

$$\theta_k = (-1)^k \frac{\xi_k}{F}, \tag{6}$$

and the beam offset at the end of the linac is

$$x_N = \sum_{k=1}^{N-1} R_{Nk} (-1)^k \frac{\xi_k}{F}. \tag{7}$$

For the variance of x_N we have

$$\langle x_N^2 \rangle = \frac{1}{F^2} \sum_{k,l=1}^{N-1} R_{Nk} R_{Nl} (-1)^{k+l} \langle \xi_k \xi_l \rangle. \tag{8}$$

Since ξ_i are assumed uncorrelated, $\langle \xi_k \xi_l \rangle = \langle \xi^2 \rangle \delta_{kl}$, where $\langle \xi^2 \rangle$ denotes the variance of the random variables ξ_i. Then Eq. (8) reduces to

$$\langle x_N^2 \rangle = \frac{\langle \xi^2 \rangle}{F^2} \sum_{l=1}^{N-1} R_{Nl}^2. \tag{9}$$

To calculate the sum in Eq. (9), we use the complex representation of Eq. (5),

$$\sum_{l=1}^{N-1} R_{Nl}^2 = -\frac{1}{4}\beta_N \sum_{l=1}^{N-1} \beta_l \left(e^{\frac{1}{2}i\mu(N-l)} - e^{-\frac{1}{2}i\mu(N-l)}\right)^2. \tag{10}$$

In the limit $N \gg 1$, the leading term in the sum will be given by the cross term in the brackets that does not contain the oscillating exponent $\exp[\pm\frac{1}{2}i\mu(N-l)]$,

$$-\sum_{l=1}^{N-1} \beta_l (e^{\frac{1}{2}i\mu(N-l)} - e^{-\frac{1}{2}i\mu(N-l)})^2 \approx \sum_{l=1}^{N} 2\beta_l \approx N(\beta_{\max} + \beta_{\min}). \tag{11}$$

Hence,

$$\frac{\langle x_N^2 \rangle}{\beta_N} = \frac{N\langle \xi^2 \rangle}{4F^2}(\beta_{\max} + \beta_{\min}) = \frac{Nl\langle \xi^2 \rangle}{2F^2 \sin\mu} = 4N\frac{\langle \xi^2 \rangle}{l}\tan\frac{\mu}{2}. \tag{12}$$

We see that the rms value $\langle x_N^2 \rangle^{1/2}$ scales as $N^{1/2}$, which is a characteristic feature of the random walk motion.

As an illustration of the presented derivation, Fig. 2 shows a comparison of the result of a computer simulation with the analytical formula Eq. (12) for three lattices with different phase advance μ. In the simulation, the quadrupoles in the lattice were randomly misaligned and the orbit was calculated using Eq. (7). The simulated orbits where averaged over 100 random seeds.

In a similar fashion, one can find the rms angular spread orbits $\langle x'^2_N \rangle^{1/2}$ at the end of the linac. Starting from the general expression

$$x'_N = \sum_{k=1}^{N} G_{Nk}(-1)^{k-1}\frac{\xi_k}{F}, \tag{13}$$

and performing the same averaging as for derivation of Eq. (12), one finds

$$\langle x'^2_N \rangle = \frac{\langle x_N^2 \rangle}{\beta_N^2}, \tag{14}$$

where $\langle x_N^2 \rangle$ is given by Eq. (12).

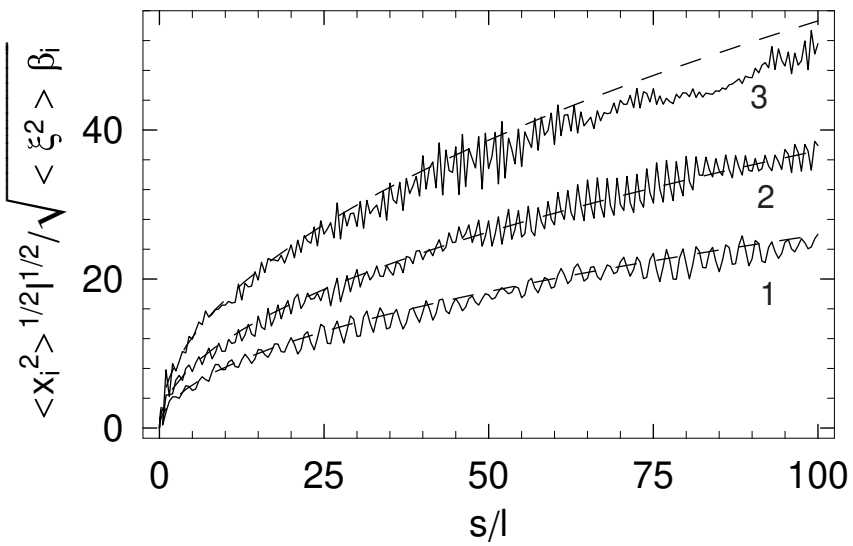

Figure 2: Beam orbit $\langle x_i^2 \rangle^{1/2}$ normalized by the quantity $\langle \xi^2 \rangle^{1/2} \beta_i^{1/2} / l^{1/2}$ at the location of ith quadrupole as a function of the distance s along the linac for FODO lattices with different phase advance μ. The simulations were performed for $\mu = 80$, (curve 1) 120 (curve 2) and 150 (curve 3) degrees with the averaging over 100 random seeds. Solid lines represent the simulation results, and the dashed curves are the corresponding theoretical predictions according to Eq. (12).

4 Chromatic Emittance Growth

When the beam has a nonzero energy spread, due to the chromaticity of the lattice, the misalignments cause an effective emittance growth of the beam [3]. In this section we will calculate the emittance increase, again assuming that the beam energy E and the relative energy spread in the beam δ are constant. We will also assume that the resulting emittance growth is much smaller than the initial emittance of the beam. In this case, we can use the following formula for the final emittance growth

$$\Delta\epsilon = \frac{1}{2}\left[\frac{1}{\beta_N}\langle(\Delta x - \langle\Delta x\rangle)^2\rangle_{\xi\delta} + \beta_N\langle(\Delta x' - \langle\Delta x'\rangle)^2\rangle_{\xi\delta}\right], \qquad (15)$$

where Δx and $\Delta x'$ are the spread in the coordinate and the angle within the bunch at the and of the linac, and the angular brackets with the subscript $\xi\delta$

denote a double averaging: first, averaging over the random misalignment of the quadrupoles and then averaging over the particles with different energy in the beam. In this section, we will assume that the energy spread in the beam δ is so small, that one can use a linear approximation for calculation of Δx and $\Delta x'$, $\Delta x = \delta \cdot \partial x_N/\partial\delta$ and $\Delta x' = \delta \cdot \partial x'_N/\partial\delta$. Since we assume that the average misalignment of the quadrupoles is equal to zero, $\langle \xi_i \rangle = 0$, hence $\langle \Delta x \rangle = \langle \Delta x' \rangle = 0$. In this approximation Eq. (15) reduces to

$$\Delta\epsilon = \frac{1}{2}\overline{\delta^2}\left[\frac{1}{\beta_N}\left\langle\left(\frac{\partial x_N}{\partial\delta}\right)^2\right\rangle + \beta_N\left\langle\left(\frac{\partial x'_N}{\partial\delta}\right)^2\right\rangle\right]. \qquad (16)$$

where $\overline{\delta^2}$ is the variance of the energy spread within the beam.

To calculate $\partial x_N/\partial\delta$ and $\partial x'_N/\partial\delta$ we need to take the derivatives of Eqs. (7) and (13) with respect to δ. For a long linac, the dominant contribution to $\Delta\epsilon$ comes from the dependence of the phase advance $\Delta\psi_{ik}$ versus energy, so we need to differentiate only $\sin\Delta\psi_{ik}$ (or $\cos\Delta\psi_{ik}$) terms in the sum,

$$\begin{aligned}\frac{\partial x_N}{\partial\delta} &\approx \sum_{k=1}^{N-1}\frac{\partial R_{Nk}}{\partial\delta}(-1)^k\frac{\xi_k}{F} \\ &\approx \sum_{k=1}^{N-1}\sqrt{\beta_N\beta_k}(-1)^k\frac{\xi_k}{F}\frac{1}{2}(N-k)\frac{\partial\mu}{\partial\delta}\cos\left(\frac{1}{2}(N-k)\mu\right), \qquad (17)\end{aligned}$$

where we neglected the energy dependence of β_N, β_k and F. As is well known, for the FODO lattice, $\partial\mu/\partial\delta = -2\tan(\mu/2)$. Using the relation $\langle \xi_k\xi_l \rangle = \langle \xi^2 \rangle \delta_{k,l}$, for the first term in Eq. (16) we find

$$\left\langle\left(\frac{\partial x_N}{\partial\delta}\right)^2\right\rangle = \beta_N\frac{\langle\xi^2\rangle}{F^2}\tan^2\frac{\mu}{2}\sum_{k=1}^{N-1}\beta_k(N-k)^2\cos^2\left(\frac{1}{2}(N-k)\mu\right). \qquad (18)$$

Similar to the derivation of $\langle x_N^2 \rangle$ in the previous section, using the relation $\cos^2\Delta\psi_{Nk} = \frac{1}{2} + \frac{1}{2}\cos 2\Delta\psi_{Nk}$, one can show that the oscillating term in this expression gives a small contribution to the sum, so that effectively we can substitute $\cos^2\frac{1}{2}(N-k)\mu \to 1/2$. Then the beta function β_k, can be substituted by its average value in the lattice, $\beta_k \to (\beta_{\max} + \beta_{\min})/2$. Finally, because N is a large numver, the summation of the term $N-k$ can be approximated by integration, $\sum_{k=1}^{N-1}(N-k)^2 \to \int_0^N (N-k)^2 dk = N^3/3$. Combining all the terms, one finds

$$\frac{1}{\beta_N}\left\langle\left(\frac{\partial x_N}{\partial\delta}\right)^2\right\rangle = \frac{4}{3}N^3\frac{\langle\xi^2\rangle}{l}\tan^3\frac{\mu}{2}. \qquad (19)$$

Similarly, one can find the second term in Eq. (16),

$$\beta_N \left\langle \left(\frac{\partial x'_N}{\partial \delta} \right)^2 \right\rangle = \frac{4}{3} N^3 \frac{\langle \xi^2 \rangle}{l} \tan^3 \frac{\mu}{2}, \tag{20}$$

which gives for the emittance growth

$$\Delta\epsilon = \frac{4}{3} \overline{\delta^2} N^3 \frac{\langle \xi^2 \rangle}{l} \tan^3 \frac{\mu}{2}. \tag{21}$$

As we see, the increase in the emittance scales with the number of quadrupoles as N^3. As an illustration of such scaling, Fig. 3 shows a comparison of the computer simulation with the analytical formula Eq. (21).

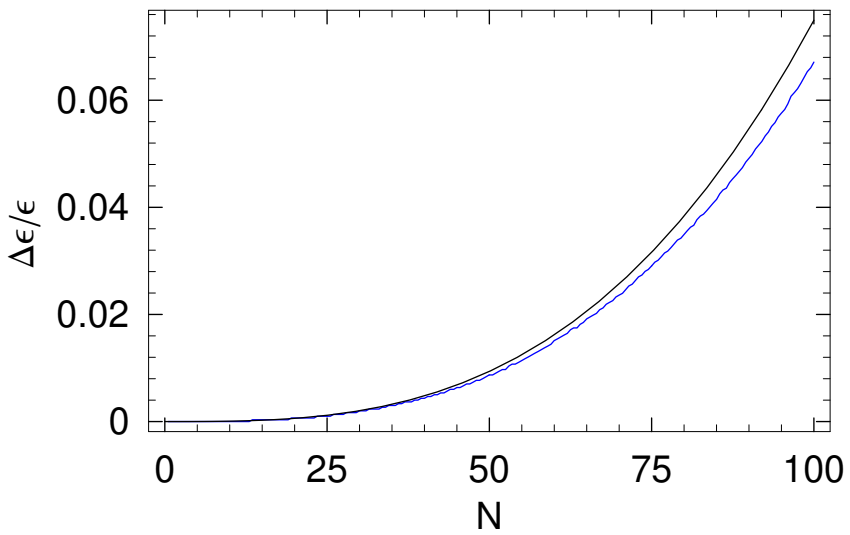

Figure 3: The relative emittance growth of a beam as a function of the length of the linac. The computer simulation (lower curve) were performed for a FODO lattice with $\mu = 80$ degrees phase advance averaged over 100 random seeds, and the beam energy spread $\delta = 10^{-4}$. The upper curve is the analytical formula (21).

In the above derivation, to find the dispersion of the beam at the end of the linac, we explicitly differentiated Eq. (7) with respect to the energy. One can use another formula for computing $\partial x_N / \partial \delta$,

$$\frac{\partial x_N}{\partial \delta} = \sum_{k=1}^{N-1} R_{Nk} (-1)^k \frac{x_k - \xi_k}{F}, \tag{22}$$

that takes into account that the dispersion is generated due to the offset of the particle relative to the center of the quadrupole, and propagates downstream with the same matrix element R_{Nk}. In Appendix A we prove, that this expression is equivalent to the approach that uses the direct differentiation of x_N. It turns out, that in the case of orbit steering (see below), it is more convenient to use Eq. (22) rather than Eq. (17).

5 Very long linac

Increasing the length of the linac and the number of quadrupoles N brings us to the regime where Eq. (21) is not valid any more. The transition occurs when the phase advance over the length of the linac due to the energy variation δ becomes comparable to $\pi/2$, $N\delta \cdot d\mu/d\delta \sim \pi/2$. In this case, the differential approximation $\Delta x = \delta \cdot \partial x_N/\partial\delta$ that was used in Section 4 becomes invalid, and the scaling $\Delta\epsilon \propto N^3$ breaks down.

A new scaling of the emittance dilution with the number of quadrupoles in the linac is illustrated by Fig. 4 which shows comparison of the computer simulated emittance growth as a function of N with the analytical formula (21). As is seen, after an initial growth $\propto N^3$, the emittance starts to grow linearly with the distance. For the case shown in Fig. 4, where $\delta = 10^{-2}$, the transition corresponds to $N \sim 10^2$.

We can estimate the emittance dilution in this regime, using the following arguments. Let us denote by l_c the decoherence length in the linac such that $(l_c/l)\delta \cdot d\mu/d\delta = \pi/2$. When the beam passes the distance l_c, due to the filamentation, the betatron oscillation of the beam are converted into the increased emittance, and the subsequent motion becomes uncorrelated with the previously excited betatron oscillations. The emittance growth on the distance l_c is given by Eq. (21), in which $N = 2l_c/l$,

$$\Delta\epsilon_c = \frac{4}{3}\overline{\delta^2}\left(\frac{2l_c}{l}\right)^3 \frac{\langle\xi^2\rangle}{l}\tan^3\frac{\mu}{2} \approx \frac{\langle\xi^2\rangle}{l\sqrt{\overline{\delta^2}}}\,. \tag{23}$$

The total emittance increase in the linac of length l_L in this regime is equal to $\Delta\epsilon_c$ multiplied by the number of coherent distances l_L/l_c in the linac

$$\Delta\epsilon = \Delta\epsilon_c\frac{l_L}{l_c} \sim \frac{l_L\langle\xi^2\rangle}{l^2\tan\frac{\mu}{2}}\,. \tag{24}$$

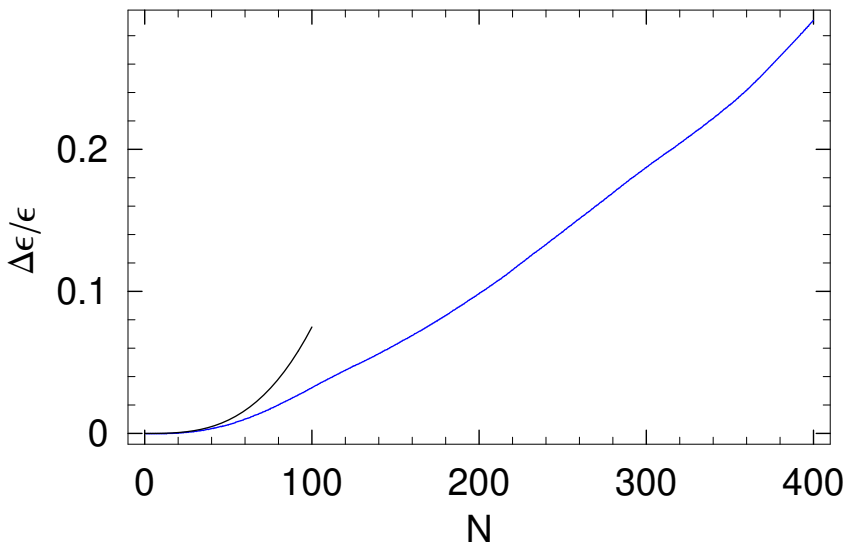

Figure 4: The relative emittance growth of a beam as a function of N in a long linac. The computer simulation (lower curve) were performed for a FODO lattice with $\mu = 80$ degrees phase advance averaged over 100 random seeds, and the beam energy spread $\delta = 10^{-2}$. The rms value of the misalignments in this case is 100 times smaller than in the simulation shown in Fig. 3. The upper curve is the analytical formula (21).

Note that if the linac length $l_L < l_c$, the emittance dilution is reversible in principle – the initial beam emittance can be recovered by taking out the dispersion generated by the misaligned quadrupoles downstream of the linac. For very long linacs, when $l_L > l_c$, the emittance growth becomes irreversible due to the phase space filamentation, and associated with it decoherence of the betatron oscillations.

6 Alignment with account of BPM errors and finite mover steps

Measuring the beam position at each quadrupole, with the knowledge of the lattice functions, allows us to find the quadrupole offsets ξ_i. Moving the quadrupoles by distance $-\xi_i$ would position them in the original state, and

restore the ideal lattice. Of course, in reality, there are many factors, such as wakefields and measurement errors, that do not allow to perfectly align the lattice. In this section we will study two such effects – errors associated with the BPM measurements, and finite step of the quadrupole movers that, even with the perfect knowledge of the values ξ_i, do not allow to move the quadrupoles exactly to the desired place.

Let us consider first the effect of BPM errors. Due to the finite resolution of BPMs the measured vector of the beam transverse offsets $X^M = (x_1^M \dots x_N^M)$ differs from the exact values $X = (x_1 \dots x_N)$ by an error vector e, $X^M = X + e$, where $e = (e_1 \dots e_N)$. The errors are small relative to the measured values, $|e_i| \ll |x_i|$. We assume that the BPMs are built in the quadrupoles, and the quadrupole displacement ξ_k also moves the center line of the BMP, so that BPM reading is

$$x_k^M = x_k - \xi_k + e_k. \tag{25}$$

Using the measured offsets x_k^M we infer the quadrupole offsets ζ_k from the following equation

$$x_i^M + \zeta_i = \sum_{k=1}^{i-1} R_{ik}(-1)^k \frac{\zeta_k}{F}. \tag{26}$$

Note that without errors, $e_k = 0$, we would find from Eq. (26) the correct value $\zeta_k = \xi_k$. Measurement errors e_k cause the inferred values of the offsets differ from the true ones, $\zeta_k \neq \xi_k$.

We then align the lattice by moving the quadrupoles by distance $-\zeta_k$. After the alignment the corrected beam orbit $\tilde{x}_i$ does not vanish:

$$\tilde{x}_i = \sum_{k=1}^{i-1} R_{ik}(-1)^k \frac{\xi_k - \zeta_k}{F} = x_i - x_i^M - \zeta_i = -e_i + \xi_i - \zeta_i. \tag{27}$$

Since the quadrupoles after alignment are located at $\xi_k - \zeta_k$, the beam offset *relative to the center of the quadrupole*, $\tilde{x}_k - (\xi_k - \zeta_k)$, is equal to $-e_k$. This important observation allows us to use Eq. (22) to find the emittance dilution in the linac after the alignment,

$$\frac{\partial x_N}{\partial \delta} = -\sum_{k=0}^{N-1} R_{Nk}(-1)^{k-1} \frac{e_k}{F}. \tag{28}$$

Assuming that e_k are uncorrelated random numbers makes the problem

equivalent to the orbit equation (7) with the result given by Eq. (12),

$$\frac{1}{\beta_N}\left\langle\left(\frac{\partial x_N}{\partial\delta}\right)^2\right\rangle = 4N\frac{\langle e^2\rangle}{l}\tan\frac{\mu}{2}. \tag{29}$$

We see that the rms value of the dispersion at the and of the linac after alignment scales as $\sqrt{N}$. Calculating in a similar way the variance of the derivative $\partial x'_N/\partial\delta$, allows us to find the chromatic emittance growth after alignment,

$$\Delta\epsilon = 4N\overline{\delta^2}\frac{\langle e^2\rangle}{l}\tan\frac{\mu}{2}\,. \tag{30}$$

Let us now assume that in addition to the BPM errors the quadrupole movers have a finite step so that the final position of the quadrupoles ζ_k after alignment is $\xi_k - \zeta_k + r_k$, where as above, ζ_k is the offset inferred from the measurements (and containing BPM errors), and r_k is the quadrupole movement error. Again, we assume that r_k are random, uncorrelated numbers, and of course uncorrelated with the BPM errors e_k. For the beam orbit after alignment we now have

$$\tilde{x}_i = -e_i + \xi_i - \zeta_i + \sum_{k=1}^{i-1} R_{ik}r_k \tag{31}$$

with the resulting emittance growth that is a combination of Eqs. (30) and (21),

$$\Delta\epsilon = 4N\overline{\delta^2}\frac{\langle e^2\rangle}{l}\tan\frac{\mu}{2} + \frac{4}{3}\overline{\delta^2}N^3\frac{\langle r^2\rangle}{l}\tan^3\frac{\mu}{2}\,. \tag{32}$$

From this equation, it follows that for a large N, the contribution of the movers errors becomes more important and imposes tighter tolerances on the movers.

7 Varying parameters of lattice and beam

In the previous section we assumed that such parameters of the lattice, as phase advance μ and the cell length l are constant throughout the linac. We also assumed that the beam energy E, and the energy spread δ are constant. In reality however, this is not true: the energy of the beam increases during acceleration, and the energy spread changes along the orbit. Also, the lattice

parameters often vary along the linac. In this section, we generalize our approach and take those variations into account.

We now assume that the lattice can be characterized as a local FODO, that is μ and l are defined in each cell of the lattice but can slowly vary with s. We also allow a slow variation of the beam parameters γ and δ. Finally, the variance of the misalignment $\langle \xi^2 \rangle$ can now be a slow function of s. The slow variation of the parameters, allows us to average out the oscillating terms in the corresponding sums, as in the case of constant parameters, leaving only the secular terms.

First, we need to generalize the expressions (2) and (4) for the transfer matrix elements for the case when the beam energy is not constant. In case of acceleration we have

$$R_{ik} = \sqrt{\frac{\gamma_k}{\gamma_i}} \sqrt{\beta_i \beta_k} \sin \Delta\psi_{ik}, \qquad G_{ik} = \sqrt{\frac{\gamma_k \beta_k}{\gamma_i \beta_i}} \cos \Delta\psi_{ik}, \tag{33}$$

where we again assumed that the parameter α is equal to zero in both initial and final points[1]. With these definitions, we can repeat the derivation of Section 3 using the fact that the main contribution comes from the nonoscillating terms in the sum. For the variance of the orbit deviation one now finds

$$\frac{\gamma_N \langle x_N^2 \rangle}{\beta_N} = \gamma_N \beta_N \langle x'^2_N \rangle = 4 \sum_{\mathrm{k}} \frac{\gamma_k \langle \xi_k^2 \rangle}{l_k} \tan \frac{\mu_k}{2}. \tag{34}$$

As pointed out at the beginning of this Section, in this expression, all parameters under the sum sign can slowly vary along the linac. Eq. (34) demonstrates the effect of adiabatic damping of the betatron oscillations during acceleration.

A similar generalization can be done for the chromatic emittance growth in the misaligned lattice. The complication here comes from the fact that the phase advance $\Delta\psi_{ik}$ is now equal to

$$\Delta\psi_{ik} = \sum_{l=k}^{i} \mu_l \tag{35}$$

and the variation of the phase advance gives

$$\delta\Delta\psi_{Ni} = \sum_{l=i}^{N} \delta_l \frac{d\mu_l}{d\delta} = 2 \sum_{l=i}^{N} \delta_l \tan \frac{\mu_l}{2} \tag{36}$$

[1]Note that now this parameter should be defined as $\alpha = -\frac{1}{2}\gamma d(\beta/\gamma)/ds$.

This gives the following result for the normalized emittance growt

$$\gamma_N \Delta\epsilon = 4 \sum_k s_k^2 \langle \xi_k^2 \rangle \frac{\gamma_k}{l_k} \tan \frac{\mu_k}{2} \,, \tag{37}$$

where

$$s_k = \sum_{l=i}^{k} \delta_l \tan \frac{\mu_l}{2} \,. \tag{38}$$

Finally, a generalization of Eq. (32) for the case of varying parameters reads

$$\gamma_N \Delta\epsilon = 4 \sum_k \delta_k^2 \frac{\gamma_k \langle e_k^2 \rangle}{l_k} \tan \frac{\mu}{2} + 4 \sum_k s_k^2 \langle r_k^2 \rangle \frac{\gamma_k}{l_k} \tan \frac{\mu_k}{2} \,. \tag{39}$$

where the first term is due to the finite BPM resolution, and the second term accounts for the finite mover step.

8 Analysis of the NLC lattice

Strictly speaking, the NLC lattice is not a FODO lattice with slowly varying parameters. The phase advance μ, the cell length l and the nominal rms energy spread in the beam as functions of position s for this lattice are shown in Fig. 5. As is seen, the lattice consists of three segments, which are approximately FODO, however the lattice parameters experience jumps at the boundaries of the segments. Nevertheless, we will apply the theory developed in the previous section to this lattice.

We also note here that for the NLC lattice the betatron phase advance within the bunch on the length of the linac is relatively large,

$$|\delta\mu| = 2 \sum_{k=1}^{N} \delta_k \tan \frac{\mu_k}{2} = 5.3 \,. \tag{40}$$

This means that the decoherence effects in the lattice are rather strong, and Eq. (37) tends to overestimate the emittance growth. The computer simulations were performed using the code LIAR [7] for the nominal NLC parameters: the initial beam energy – 10 GeV, the final beam energy – 500 GeV, number of particles in the bunch – $1.1 \cdot 10^{10}$. In the first set of simulations, the quadrupoles were misaligned in the vertical direction with the rms offset of 40 nm and no orbit correction was used. The transverse wakefields were turned off in the simulation. The vertical normalized emittance growth

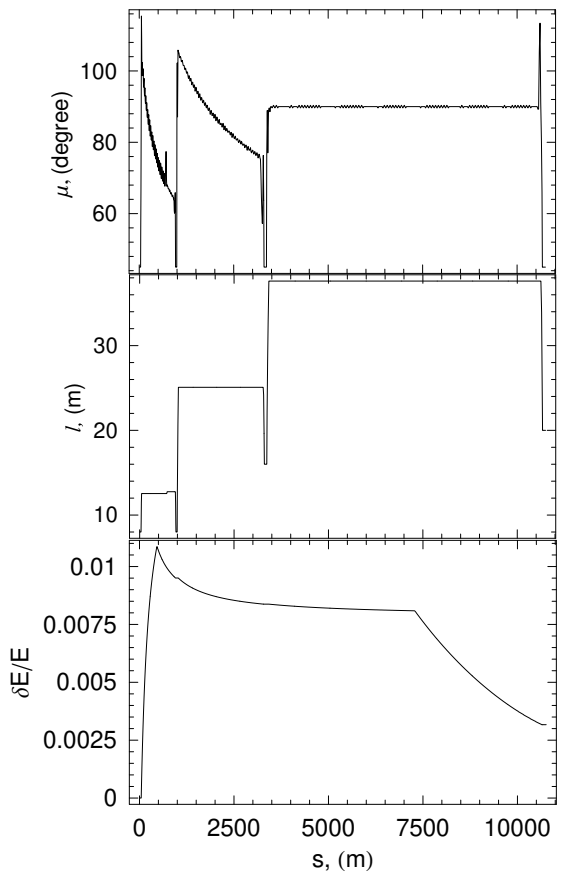

Figure 5: The NLC lattice. Shown are the phase advance μ, the cell length l and the nominal rms energy spread in the beam as functions of position s.

is shown in Fig. 6. As we see, the beam emittance doubles in this case. A theoretical estimate for the NLC lattice based on Eq. (37) with the lattice parameters and the beam energy spread shown in Fig. 5 gives the following result,

$$\gamma_N \Delta\epsilon = 2 \cdot 10^8 \langle \xi_k^2 \rangle \text{ m}^{-1}, \tag{41}$$

which for $\langle \xi_k^2 \rangle^{1/2} = 40$ nm gives $\gamma_N \Delta\epsilon = 3.2 \cdot 10^{-7}$ m, or about ten times the initial emittance. As expected, the theoretical formula overestimates the emittance growth in this case.

Another set of simulations was performed with 1 to 1 orbit steering assuming the BPM resolution of 3 μm. The result of the simulations in this

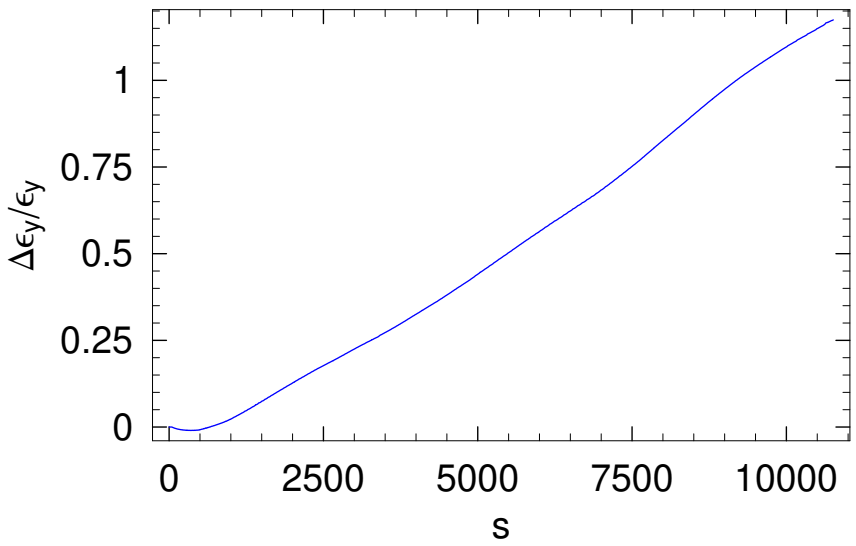

Figure 6: Vertical emittance growth for 40 nm rms misalignments. The shown result is an average value over 100 random seeds.

case is shown in Fig. 7. Again the emittance approximately doubles over the length of the linac. The theoretical formula for this case, Eq. (39), reads

$$\gamma_N \Delta\epsilon = 2 \cdot 10^3 \langle e_k^2 \rangle \text{ m}^{-1}, \tag{42}$$

which for which for $\langle e_k^2 \rangle^{1/2} = 3$ μm gives $\gamma_N \Delta\epsilon = 1.8 \cdot 10^{-8}$ m, or about half of the initial emittance. We see that in this case the theory is in qualitative agreement with the simulations.

9 Summary

We have studied the emittance growth caused by chromatic effects in the lattice with randomly misaligned quadrupoles of a long linac. The simplest problem of this kind — a FODO lattice with a beam of constant energy and constant energy spread — allows an analytical solution for both beam orbit and emittance dilution. These solutions, given by Eqs. (12) and (21), are valid for not very long linacs, such that betatron oscillations of the beam do not decohere on the linac length. In this regime, the rms orbit deviation and emittance increase scale as $N^{1/2}$ and N^3, respectively, with the number of

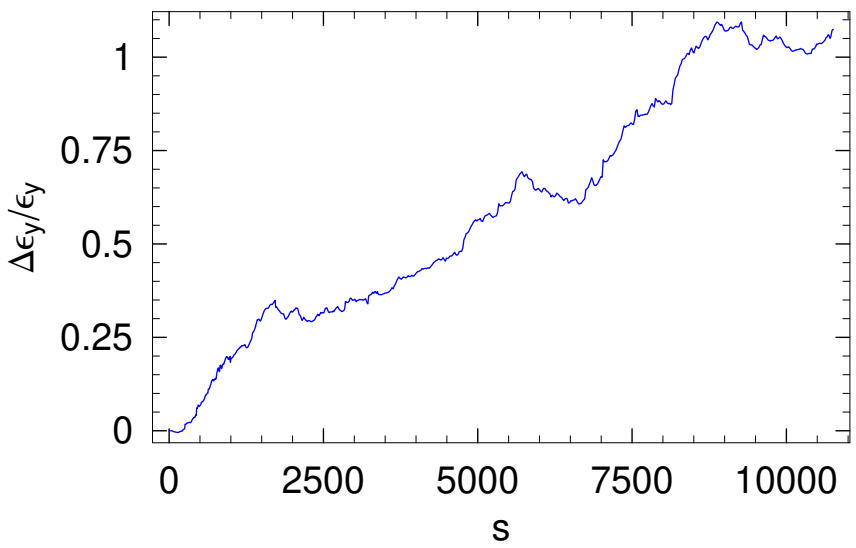

Figure 7: Vertical emittance growth for 1 to 1 orbit correction. The shown result is an average value over 100 random seeds.

quadrupoles in the linac. In the limit when the linac length is much longer than the decoherence length, the chromatic emittance dilution scales linearly with the length of the linac. Note, that for the NLC lattice the decoherence length (for the nominal relative energy spread of order of 1%) is of the order of the linac length, as estimated in Section 8, which means that the NLC is in an intermediate regime between these two limits.

We have also studied the effect of quadrupole alignment based on steering the orbit through the centers of the beam position monitors. After such alignment the residual emittance dilution caused by the finite BPM resolution scales linearly with N. However, finite movers steps add to the emittance growth a term that again scales as N^3.

We also generalized the results for the emittance growth for the case of a FODO lattice with slowly varying parameters taking also into account a slow variation of beam energy and energy spread. Those results are compared with the computer simulation for the NLC beam.

10 Acknowledgments

The author thanks A. Seryi for useful discussions.

11 Appendix A

To prove Eq. (22) we consider a differential equation of betatron oscillations in a linac with continuous focusing strength $K(s)$ and misalignments $\xi(s)$,

$$\frac{\partial^2 x}{\partial s^2} + K(s)x = K(s)\xi(s)\,. \tag{43}$$

In the limit of thin lenses, which is treated in this paper, the functions $K(s)$ reduces to a sum of delta functions, however, we do not need to use this assumption here.

Introducing the Green function $G(s,s')$ which satisfies the equation

$$\frac{\partial^2 G}{\partial s^2} + K(s)G = \delta(s-s'), \tag{44}$$

with $G(s,s') = 0$ for $s < s'$, the perturbed orbit is given by

$$x(s) = \int_0^s G(s,s')K(s')\xi(s')ds', \tag{45}$$

where $s = 0$ corresponds to the beginning of the linac.

To find the derivative of the orbit with respect to δ we differentiate Eq. (45)

$$\frac{\partial x(s)}{\partial \delta} = \int_0^s \left[G_\delta(s,s')K(s') + G(s,s')K_\delta(s')\right]\xi(s')ds'. \tag{46}$$

The derivative of the focusing strength with respect to the relative energy is $K_\delta = -K$. For the derivative G_δ, we will use a differential equation that is obtained by differentiating Eq. (44)

$$\frac{\partial^2 G_\delta}{\partial s^2} + K(s)G_\delta = -K_\delta(s)G(s,s') = K(s)G(s,s'). \tag{47}$$

The solution to the last equation can be found using the Green function

$$G_\delta(s,s') = \int_{s'}^s G(s,s'')K(s'')G(s'',s')\,ds''. \tag{48}$$

Putting Eq. (48) into Eq. (46) yields

$$\begin{aligned}\frac{\partial x(s)}{\partial \delta} &= \int_0^s K(s')\xi(s')ds' \int_{s'}^s G(s,s'')K(s'')G(s'',s')ds'' \\ &- \int_0^s G(s,s')K(s')\xi(s')ds'. \end{aligned} \tag{49}$$

Changing the order of integration in the first integral gives

$$\begin{aligned}\frac{\partial x(s)}{\partial \delta} &= \int_0^s G(s,s'')K(s'')ds'' \int_0^{s''} K(s')\xi(s')G(s'',s')ds' \\ &- \int_0^s G(s,s')K(s')\xi(s')ds' \\ &= \int_0^s x(s'')G(s,s'')K(s'')ds'' - \int_0^s G(s,s')K(s')\xi(s')ds' \\ &= \int_0^s G(s,s')K(s')(x(s')-\xi(s'))ds' \,. \end{aligned} \tag{50}$$

For thin quadrupoles, $K(s) = \sum_{n=1}^{N}(-1)^n F^{-1}\delta(s-s_n)$, where $s_n = (n-1)l/2$, and Eq. (50) reduces to Eq. (22) with $x_N = x(s_N)$ and $R_{ik} = G(x_i, x_k)$.

References

[1] V. E. Balakin, A. V. Novokhatsky, and V. P. Smirnov, in F. T. Cole and R. Donaldson, eds., *Proc. International Conference on High-Energy Accelerators, Batavia, 1983* (Fermi National Accelerator Lab., Batavia, IL, 1984), pp. 119–120.

[2] The NLC Design Group, *Zeroth-Order Design Report for the Next Linear Collider*, Report SLAC-474, Stanford Linear Accelerator Center, Stanford, CA, USA (May 1996).

[3] R. D. Ruth, in *US/CERN Joint Topical Course on "Frontiers of Particle Beams"* (1987), pp. 440–460.

[4] T. O. Raubenheimer and R. D. Ruth, Nucl. Instrum. Meth. **A302**, 191 (1991).

[5] A. Sery and O. Napoly, Phys. Rev. **E53**, 5323 (1996).

[6] A. Sery and A. Mosnier, Phys. Rev. **E56**, 3558 (1997).

[7] R. Assmann, C. Adolphsen, K. Bane, P. Emma, T. Raubenheimer, R. Siemann, K. Thompson, and F. Zimmermann, *LIAR: a computer program for the modeling and simulation of high performance linacs*, Tech. Rep. SLAC-AP-103, SLAC (April 1997).